

Applications of direct injection soft chemical ionisation-mass spectrometry for the detection of pre-blast smokeless powder organic additives

González-méndez, Ramón; Mayhew, Chris A.

DOI:

[10.1007/s13361-018-02130-1](https://doi.org/10.1007/s13361-018-02130-1)

License:

Other (please specify with Rights Statement)

Document Version

Peer reviewed version

Citation for published version (Harvard):

González-méndez, R & Mayhew, CA 2019, 'Applications of direct injection soft chemical ionisation-mass spectrometry for the detection of pre-blast smokeless powder organic additives', *Journal of the American Society for Mass Spectrometry*, vol. 30, no. 4, pp. 615-624. <https://doi.org/10.1007/s13361-018-02130-1>

[Link to publication on Research at Birmingham portal](#)

Publisher Rights Statement:

The final publication is available at Springer via <https://doi.org/10.1007/s13361-018-02130-1>

González-Méndez, R. & Mayhew, C.A. J. Am. Soc. Mass Spectrom. (2019). <https://doi.org/10.1007/s13361-018-02130-1>

General rights

Unless a licence is specified above, all rights (including copyright and moral rights) in this document are retained by the authors and/or the copyright holders. The express permission of the copyright holder must be obtained for any use of this material other than for purposes permitted by law.

- Users may freely distribute the URL that is used to identify this publication.
- Users may download and/or print one copy of the publication from the University of Birmingham research portal for the purpose of private study or non-commercial research.
- User may use extracts from the document in line with the concept of 'fair dealing' under the Copyright, Designs and Patents Act 1988 (?)
- Users may not further distribute the material nor use it for the purposes of commercial gain.

Where a licence is displayed above, please note the terms and conditions of the licence govern your use of this document.

When citing, please reference the published version.

Take down policy

While the University of Birmingham exercises care and attention in making items available there are rare occasions when an item has been uploaded in error or has been deemed to be commercially or otherwise sensitive.

If you believe that this is the case for this document, please contact UBIRA@lists.bham.ac.uk providing details and we will remove access to the work immediately and investigate.

Applications of Direct Injection Soft Chemical Ionisation-Mass Spectrometry for the Detection of Pre-blast Smokeless Powder Organic Additives

Ramón González-Méndez^{1,2*} and Chris A. Mayhew^{1,3}

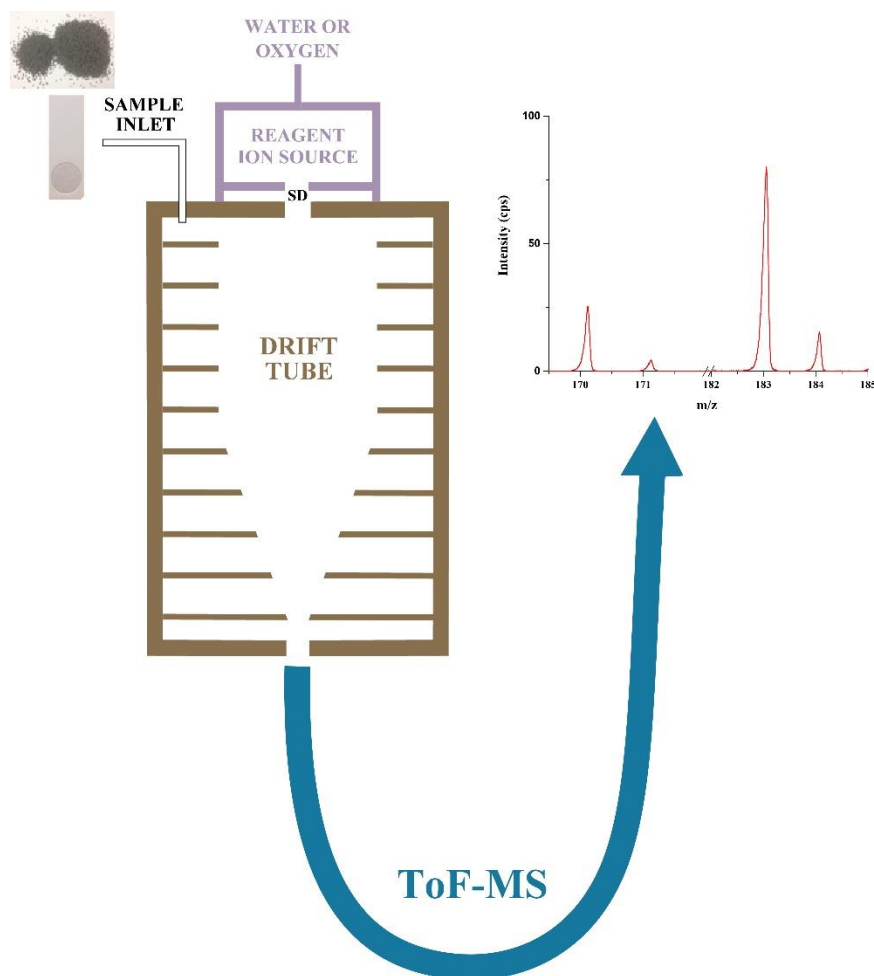
1. Molecular Physics Group, School of Physics and Astronomy, University of Birmingham, Edgbaston, Birmingham, B15 2TT, UK
2. Centre for Agroecology, Water and Resilience, Coventry University, Coventry, CV1 5FB, UK
3. Institut für Atemgasanalytik, Leopold-Franzens-Universität Innsbruck, Rathausplatz 4, A-6850 Dornbirn, Austria

*Corresponding Author Tel.: +44 247 7651678.

E-mail: R.GonzalezMendez@bham.ac.uk / Ramon.Gonzalez-Mendez@coventry.ac.uk

Key words: Soft Chemical Ionisation-Mass Spectrometry; SCIMS; Proton Transfer Reaction Mass Spectrometry; PTR-MS; Smokeless Powders; Smokeless Powder Additives

Graphical Abstract



Research highlights

- **Use of Direct Injection Soft Chemical Ionisation-Mass Spectrometry for smokeless powder organic additives analysis**
- **Study of the underlying water and oxygen chemistry in positive ion mode**
- **Comparison of fragmentation patterns for H_3O^+ and O_2^+ reagent ions**
- **Performance evaluation for the method in terms of sensitivity, linear dynamic range and precision**
- **Application to commercial pre-blast samples**

Abstract

Analysis of smokeless powders is of interest from forensics and security perspectives. This article reports the detection of smokeless powder organic additives (in their pre-detonation condition), namely the stabiliser diphenylamine and its derivatives 2-nitrodiphenylamine and 4-nitrodiphenylamine, and the additives (used both as stabilisers and plasticisers) methyl centralite and ethyl centralite, by means of swab sampling followed by thermal desorption and Direct Injection Soft Chemical Ionisation-Mass Spectrometry. Investigations on the products resulting from the reactions of the reagent ions H_3O^+ and O_2^+ with additives as a function of reduced electric field are reported. The method was comprehensively evaluated in terms of linearity, sensitivity and precision. For H_3O^+ , the limits of detection (LoD) are in the range of 41-88 pg of additive, for which the accuracy varied between 1.5-3.2%, precision varied between 3.7-7.3% and linearity showed $R^2 \geq 0.9991$. For O_2^+ , LoD are in the range of 72 pg to 1.4 ng, with an accuracy of between 2.8-4.9% and a precision between 4.5-8.6% and $R^2 \geq 0.9914$. The validated methodology was applied to the analysis of commercial pre-blast gun powders from different manufacturers.

1. Introduction

Smokeless powders are a large and complex family of products used as propellants in ammunition cartridges,¹ categorized as low explosives (they burn rapidly instead of detonating).² They are commonly employed in forensic analyses as their residues can be used as evidence for firearms discharge.^{3,4} They are also relevant from a Homeland Security perspective, as they are readily available and can be employed in the manufacturing of improvised explosive devices (IEDs).⁵ They exhibit a complex composition, consisting of an explosive material (nitrocellulose, nitroglycerin, nitroguanidine or different mixtures of them),¹ heavy metals,^{1,6} and a large number of different classes of organic compounds.^{1,7,8} The latter became of great interest after the introduction of heavy-metal free ammunition in the market.³ Within the organic additives category we can include plasticizers, stabilisers, opacifiers, flash suppressants, coolants, surface lubricants and dyes.^{2, 9-13} The aim of these additives is to increase the shelf-life and modify the burning characteristics of the powder.^{5,14} Different concentrations and/or different additives are characteristic of a given manufacturer, producing therefore a chemical fingerprint for each powder.¹⁵ It is thus also important to determine their content throughout the manufacturing quality control process. Among all the possible additives there are a number of key chemicals usually present and regarded as characteristic of smokeless powders.^{1,12,16} The most common are the stabiliser diphenylamine (DPA) and its derivatives 2-nitrodiphenylamine (2-NO₂-DPA) and 4-nitrodiphenylamine (4-NO₂-DPA), and the additives (used both as stabilisers and plasticisers) methyl centralite (MC) and ethyl centralite (EC), which are the subject of this current paper - for structural information see table 1.

Several analytical techniques have been used for the qualitative and/or quantitative detection of smokeless powders, either in their pre and/or post-blast forms,^{9,10} including High-Performance Liquid Chromatography (HPLC),¹⁷⁻¹⁹ Liquid Chromatography-Mass Spectrometry (LC-MS),^{8,20-22} Fourier Transform Infrared Spectroscopy,²³ Gas Chromatography (GC),^{12,14,24} Capillary Electrophoresis (CE),^{25,26} Ion Mobility Spectrometry (IMS),²⁷ Solid Phase Microextraction-Ion Mobility Spectrometry (SPME)-IMS,^{12,28} (Nano)Electrospray Ionization (nESI)-Tandem Mass Spectrometry,²⁹⁻³¹ Laser Electrospray-Mass spectrometry (LEMS),^{15,32} Desorption Electrospray Ionization-Mass spectrometry (DESI),^{33,34} Direct Analysis in Real Time- Mass Spectrometry (DART-MS),³⁵ Time-of-Flight Secondary Ion-Mass Spectrometry (ToF-MS),³⁶ and Raman Spectroscopy.^{23,37} Most of the above-mentioned techniques require time-consuming sample preparation step(s) - exception of DESI and DART; or if not, they require complicated set-ups, such the use of lasers as the means for sample vaporization (LEMS) or heated purified gases (DART). Here is where Direct

Injection (DI) Soft Chemical Ionisation-Mass Spectrometry (SCIMS) can compete (and/or be complementary) with these techniques for rapid, selective and sensitive detection of chemical compounds in complex environments. DI-SCIMS is an analytical technique for mass spectrometric gas analysis based on the ionization of neutrals by ion/molecule reactions with a reagent ion (such as H_3O^+ , O_2^+ or NO^+). This occurs within the controlled environment of a drift tube (DT) under the effect of an electric field E . The resulting ionised analyte molecules are then mass analysed by mass spectrometer. It is a direct injection technique as samples are injected directly into the drift tube of the instrument.

There are several analytical techniques that belong to the DI-SCIMS category,^{38,39} with Proton Transfer Reaction-Mass Spectrometry (PTR-MS) arguably the most widespread. PTR-MS was purposely design for the monitoring of volatile organic compounds (VOCs),⁴⁰ but has developed further to analyse liquid and solid compounds,³⁸ being successfully applied to the detection of explosives and explosive-related compounds in positive ion mode.⁴¹⁻⁵⁰ Technically speaking, PTR-MS only refers to the use of hydronium as the reagent ion. Given that in this study we investigated reactions involving O_2^+ and H_3O^+ the term SCIMS is a more accurate description of the instrument for this work.

In this paper we report the first DI-SCIMS studies of the additives to smokeless powders; namely DPA, 2- NO_2 -DPA, 4- NO_2 -DPA, MC and EC, using H_3O^+ and O_2^+ as the reagent ions. We can expect efficient reactions with H_3O^+ because the proton affinities for amine and amide-based compounds are higher than that of water. Certainly studies involving ESI-MS,³¹ and IMS,⁵¹ show that these neutrals can be detected with a high sensitivity. Based on the identified ions, analytical figures of merit (limits of detection, linear dynamic range, repeatability and reproducibility) are established. This information should help in the development of a highly selective analytical technique for smokeless powders organic additives detection using DI-SCIMS.

2. Experimental Details

2.1. Proton Transfer Reaction Mass Spectrometry (PTR-MS)

A Kore Technology Ltd. Series I PTR-ToF-MS instrument was used. Details of using PTR-MS is given in detail elsewhere,^{38,47} and therefore only pertinent issues will be briefly mentioned here. Recently this instrument was equipped with a radio frequency ion funnel drift tube and fast reaction region reduced electric field, E/N , switching capabilities.⁵⁰ However, for these studies the RF operation was not used.

2.1.1 Fast reduced electric field switching

Details of the fast switching have been given elsewhere.⁵⁰ In brief, this new hardware development feature allows the rapid switching of the reduced electric field with transition times less than 140 ms (0.1-5 Hz) within the reaction region. This alters the reagent ion composition and ion-molecule collisional energies, leading to differences in product ions between the two operational E/N values. This new hardware development allows for the manipulation of the ion-chemistry, modifying the product ion distribution to provide more information to aid in assignment of the neutral responsible for the observed product ion(s).

2.1.2 H_3O^+ production

Water vapour is introduced into a hollow cathode glow discharge where, after ionisation via electron impact and subsequent ion-molecule processes, the terminal reagent ion is H_3O^+ . These ions are transferred from the ion source into the drift tube by an applied voltage gradient where they react with the analyte M by donating their protons at the collisional rate, providing M has a proton affinity greater than that of water ($\text{PA}(\text{H}_2\text{O}) = 691 \text{ kJ mol}^{-1}$). This process can be either non-dissociative (resulting in the protonated molecule MH^+) and/or dissociative. Dissociative proton transfer results in product ions, which depending on their m/z values, may be useful for the identification of a compound. Fragmentation may be spontaneous upon proton transfer or may require additional energy which is supplied through collisions with the buffer gas resulting during the migration of ions under the influence of the electric field, E . Ions are separated using a time of flight mass analyser and detected by means of a multichannel plate. O_2^+ is also formed as an impurity due to air back flow from the reactor into the ion source region,⁴³ however the instrument was operated in a manner that this was below 2% of the H_3O^+ signal intensity.

2.1.3 O_2^+ production

For the production of O_2^+ , water vapour in the discharge is replaced by pure oxygen (99.998% purity, BOC Gases, Manchester, UK). This leads to the formation of mainly O_2^+ reagent ions (> 95%).⁵³ Once injected into the DT, O_2^+ reacts with the analyte M via charge transfer, provided that the ionisation potential of M is less than that of O_2 .⁵⁴ Similarly to 2.1.2, this reaction may be non-dissociative and/or dissociative, and fragmentation may be spontaneous upon charge transfer or require additional energy. H_3O^+ is also observed due to residual water vapour in the system, with signal intensity below around 2.5% of the O_2^+ signal for the experimental conditions used throughout.

It is worth to highlight that when using O_2^+ as the reagent ion, it is possible to start measurements at lower E/N values than when using H_3O^+ . This is a consequence of the lack of water clustering for O_2^+ . This reagent ion signal had to be inferred from its corresponding isotopologue $^{16}\text{O}^{18}\text{O}$ at m/z 33.99, owing to detection saturation at m/z 31.99.

2.2. Operational parameters

A thermal desorption unit (TDU) connected to the inlet of the drift tube through passivated (Silconert[®]) stainless steel (10 cm length), was used to introduce the samples. Details of the TDU have been given elsewhere.⁴¹ The TDU, connecting lines and drift tube were operated at a temperature of 150°C (maximum possible temperature). PTFE swabs (ThermoFisher Scientific, Cheshire, UK) onto which known quantities of additives were deposited were placed into the TDU. For this study laboratory air was used as the carrier gas. Prior to making contact with the swab, the carrier gas was passed through an oxygen/moisture trap (Agilent OT3-4) - not used for O_2^+ mode- and hydrocarbon trap (Agilent HT200-4). Upon closure of the TDU a seal is created, and the carrier gas is heated to the temperature of the TDU before it flows through a series of apertures in the heated metal plate. This heated air then passes through the swab and into the inlet system driving any desorbed material through to the drift tube creating a temporal concentration “pulse” of typically between 10-20 seconds of an analyte in the drift tube.⁴¹ For the product ion distribution and branching ratio studies each swab provided one measurement, which was replicated three times and then the results were averaged and any background signals were subtracted.

The drift tube was maintained at a pressure of 1.1 mbar and the glow discharge (for both water vapour and oxygen) was set at 1.3 mbar (which is a combination of the reagent neutral pressure and air back flowing from the drift tube).

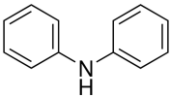
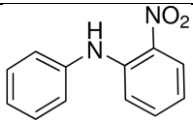
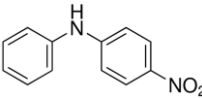
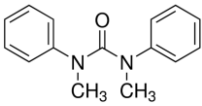
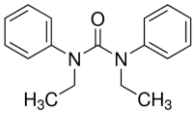
For the fast switching experiments, the acquisition time per point was set to 40 ms and ion signals were averaged for each individual cycle.

In the following only product ions with a product ion distributions (PID) greater than 1% are reported and the m/z of the lightest isotopologue will be given. However, when calculating the product ion distributions all of the isotopologues are taken into account.

2.3. Chemical standards and smokeless powder samples

Table 1 gives details of the molar mass and structure of the five compounds investigated in this study.

Table 1. Molecular weight, linear formula and chemical structure for the components investigated

Additive	Molar weight, g mol ⁻¹	Linear formula	Chemical structure
Diphenylamine (DPA)	169.22	(C ₆ H ₅) ₂ NH	
2-nitrodiphenylamine (2-NO ₂ -DPA)	214.22	C ₆ H ₅ NHC ₆ H ₄ NO ₂	
4-nitrodiphenylamine (4-NO ₂ -DPA)	214.22	C ₆ H ₅ NHC ₆ H ₄ NO ₂	
Methyl centralite (MC)	240.30	[C ₆ H ₅ N(CH ₃)] ₂ CO	
Ethylcentralite (EC)	268.35	[C ₆ H ₅ N(C ₂ H ₅)] ₂ CO	

These chemicals were individually purchased from AccuStandard Inc., (New Haven, CT, US) and used without additional treatment. DPA came dissolved in MeOH, MC and EC came prepared in a mixture of MeOH:AcN 1:1 (V/V), 2- and 4-NO₂-DPA in AcN. Concentrations in all cases were 100 µg·mL⁻¹. Further dilutions of this mother solutions in the appropriate solvent(s) (HPLC grade) were prepared when needed. Typically, 1 µL of a solution of the required concentration was spotted onto the swab and left to evaporate the solvents for 1 min prior to insertion into the TDU.

Smokeless powders (either used for guns or rifles) were acquired in a local ammunition wholesaler. Rifle powders are typically single based (the only energetic material is nitrocellulose) and gun powders are double based (nitrocellulose together with nitroglycerine). When needed, 1 g of powder was dissolved in 10 mL of dichloromethane (HPLC grade) for 10 minutes at room temperature with the help of an ultrasonic bath. Once the solvent evaporated at room temperature, the residue was dissolved in 100 mL of a mixture of MeOH:Acetonitrile 1:1 (V/V). Again, 1 µL was spotted onto the swab and left solvents to evaporate for 1 minute prior to insertion into the TDU.

3. Results and Discussion

3.1. Analysis of standard additives. Fragmentation patterns and branching ratios studies in H_3O^+ and O_2^+ modes.

3.1.1- Diphenylamine (DPA)

In H_3O^+ mode (data not shown), the protonated parent $[\text{DPA.H}]^+$ at a m/z of 170.10 dominates across the E/N range studied (80-200 Td). One other product ion is observed at high E/N values (180 Td and above) at m/z 92.05. This is assigned to $[\text{C}_6\text{H}_5\text{NH}]^+$, resulting from the loss of benzene from the protonated parent, increasing its intensity from negligible at low E/N to a maximum of 5% at 200 Td.

In O_2^+ mode (data not shown), only DPA^+ at m/z 169.09, resulting from non-dissociative charge transfer, is observed for all the E/N values (60-200 Td).

3.1.3- 2-nitrodiphenylamine (2- NO_2 -DPA) and 4-nitrodiphenylamine (4- NO_2 -DPA)

Figure 1 shows the PID plots for (a) 2- NO_2 -DPA and (b) 4- NO_2 -DPA for their reaction with H_3O^+ as a function of E/N (for the range from 80 to 200 Td). For both chemicals, the fragmentation pattern is very similar, and only differences ascribe to the *ortho* effect (**amine and nitro groups in adjacent positions for 2- NO_2 -DPA**) are observed. For both isomers the protonated parent, m/z 215.08, is the dominant ion, with the exception of the 2-isomer at E/N values above 190 Td, where a product ion at m/z 197.07 (loss of H_2O) takes over. For the 4-isomer a loss of a hydroxyl group, giving a product ion at m/z 198.08, is also observed. This is consistent with the *ortho* observed behaviour, where $[\text{M-OH}_2]^+$ replaces the $[\text{M-OH}]^+$ fragment ion.^{47,55} For the 2-isomer, a subsequent loss of an hydroxyl group (only observed at $E/N > 160$ Td) leads to the product ion at m/z 180.06, the intensity of which increases as the E/N increases. Finally, another product ion at m/z 169.07 corresponding to the nitro group loss from the protonated parent, is observed in both isomers with different intensities (maximum values of ca. 8.5% for 2-isomer and ca. 14% for the 4-isomer, at 200Td), and becoming relevant only above 150 Td in both cases.

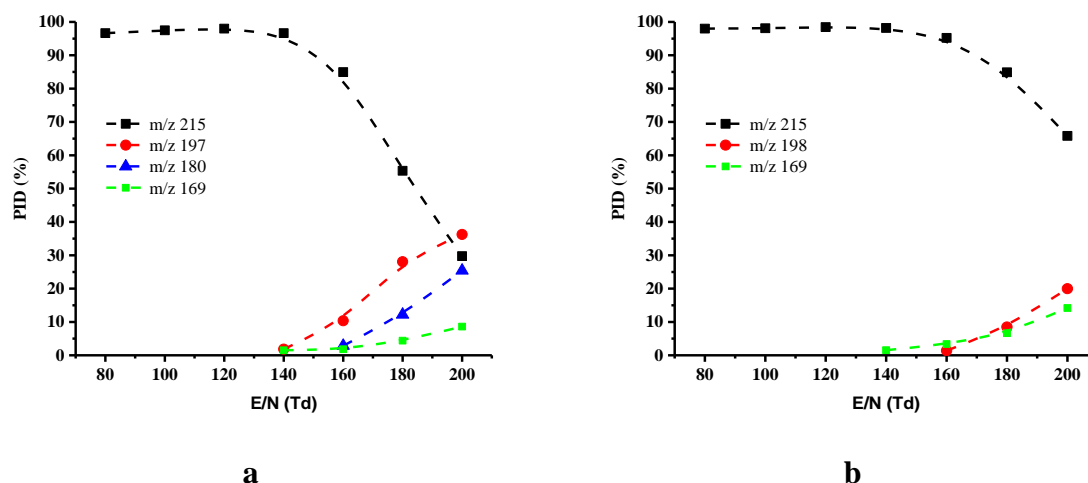


Figure 1. PID plots resulting from the reaction of H_3O^+ with (a) 2- NO_2 -DPA and (b) 4- NO_2 -DPA as a function of reduced electric field (80 to 200 Td).

In O_2^+ mode (PID plot not shown) and for both 2- and 4- NO_2 -DPA, the parent ion at m/z 214.07, the result of non-dissociative reaction channel, dominates. Its intensity decreases as the reduced electric field increases, dropping down to 25% at 180 Td of the initial intensity at 80 Td. Other fragment ion, at m/z 163.22 (unassigned in this paper), is observed in both cases, the intensity of which slightly decreases as the reduced electric field increases (from ~2% at 60 Td to 3.5% at 200 Td for 2- NO_2 -DPA, and from ~3.5% to 7% for 4- NO_2 -DPA). This unidentified ion is consistent with the observations reported by Perez et al.³²

3.1.4- Methyl centralite (MC)

In H_3O^+ mode the protonated parent at m/z 241.13, $[\text{MC.H}]^+$, is observed as the dominant ion up to around 190 Td (figure 2(a)). Other observed product ions are m/z 134.06, assigned to $[\text{PhNCH}_3\text{CO}]^+$ (resulting from the loss of *N*-methylaniline from the protonated parent), and m/z 106.07 (a subsequent loss of a CO molecule leaving a $[\text{PhNCH}_3]^+$ ion), which only yields a significant intensity above 140 Td and becomes dominant above 190 Td.

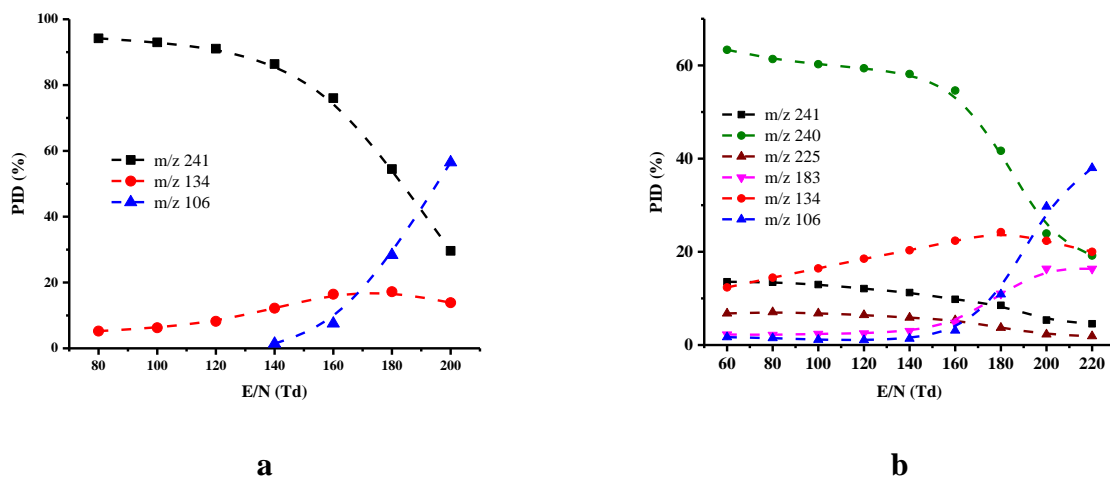


Figure 2. PID plots resulting from the reaction of MC with (a) H₃O⁺ reagent ion (80 to 200 Td) and (b) O₂⁺ reagent ion (60 to 220 Td) as a function of reduced electric field.

In O₂⁺ mode (PID shown in figure 2(b)), non-dissociative charge transfer results in an ion at *m/z* 240.12, [MC]⁺, that dominates. Only at very high *E/N* values, > ca. 200 Td, the ion at *m/z* 106.10 becomes dominant. Additional observed product ions are *m/z* 225.10 (loss of a CH₃ group) and *m/z* 183.01 (not assigned in this paper and being relevant only after 170 Td).

3.1.5- Ethyl centralite (EC)

EC has a very similar structure to that of MC, so a similar fragmentation pattern is to be expected. For water chemistry the protonated parent, [EC.H]⁺, at *m/z* 269.17, is dominant across all the *E/N* range (figure 3(a)). Observed fragment product ions are *m/z* 148.08 (via loss of *N*-ethylaniline from the protonated parent), and at *m/z* 120.08 (loss of CO), which only becomes relevant above 120 Td. Two more product ions are observed at *m/z* 93.06, assigned to be charged aniline [PhNH₂]⁺, after the additional loss of a CH₂CH molecule, and *m/z* 92.05, [PhNH]⁺, only becoming relevant at *E/N* > 140 Td. That these two ions are only and simultaneously observed for EC is consistent with results shown by Gilbert-López et al. in a LC/ESI-ToF-MS.⁵⁶

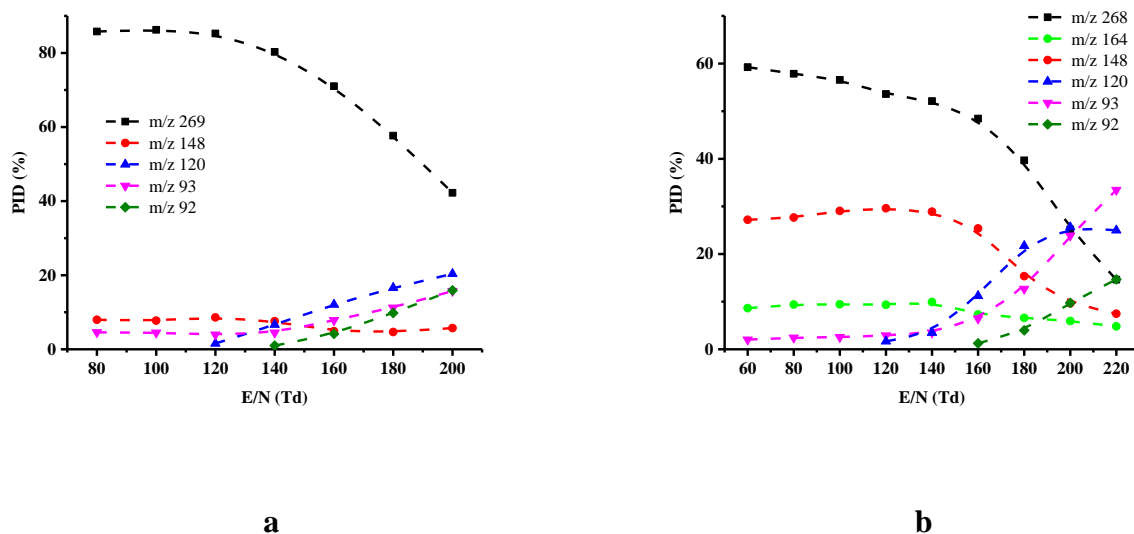


Figure 3. PID plots resulting from the reaction of EC with (a) H_3O^+ reagent ion (80 to 200 Td) and (b) O_2^+ reagent ion (60 to 220 Td) as a function of reduced electric field.

For oxygen chemistry, PID shown in figure 3(b), the ion resulting from charge transfer at m/z 268.16, dominates, and only at reduced electric field values above 200 Td loses its dominance. Identified product ions are to the same as those for water chemistry, namely m/z 148.08, 120.08, 93.06 and 92.05, but in addition another product ion at m/z 164.00 is also observed, the intensity of which remains almost constant for the range 60 to 140 Td, after which its intensity decreases to ca. 5% at 220 Td.

3.2. Method validation. Analytical figures of merit

Following the establishment of the product ions, the performance of the method was evaluated in terms of limits of detection (LoD), linear dynamic range and precision for both H_3O^+ and O_2^+ reagent ions (see table 2). Serial calibration solutions of different concentrations for each standard additive were prepared. Calibration curves, using peak areas normalised to 10^6 reagent ions, as function of concentration using least-square linear regression analysis were plotted. Instrumental LoDs were evaluated based on the minimum analyte concentration yielding to a signal to noise ratio equal to three. Noise was defined as the average of 10 blank samples for a given mass. Although the conjunction of protonated parent and fragment ions is useful for selectivity purposes, to determine the sensitivity of the method only the dominant ion resulting in the best LoD was used, i.e. the most intense ion signal (in terms of ncps) at a given E/N value was used to determine the LoD. Precision of the method was determined in terms of repeatability (measurements of 5 replicates within short intervals of time (typically 1-5 min)

by the same operator under the same experimental conditions) and reproducibility (five replicates over five different days by the same operator under the same experimental conditions), with each replicate being the mean of three measurements. Linearity was studied covering a concentration range from 0.1 to 1500 ng of each compound at ten concentration values with three replicates at each concentration. No carryover effects were observed and under the experimental conditions after ca. 10 seconds the base line was recovered for all the compounds of interest. 30 s integration time was used throughout in order to record a stable background prior and after a desorption event.

In H_3O^+ mode, the coefficient of determination R^2 was higher than 0.9991 for all compounds. Instrumental limits of detection varied from 41 to 88 pg. Precision, expressed in terms of relative standard deviation (RSD), was found in all cases to be below around 3% for intra-day (repeatability) and below 7% for inter-day (reproducibility) studies.

In O_2^+ mode, the coefficient of determination R^2 was higher than 0.9914 for all compounds. Instrumental limits of detection varied from 72 pg to 1.4 ng. Special mention should be noted to the cases of DPA, where the existence of an endogenous high background signal at the m/z of interest led to a LoD much higher than that of the rest of compounds, but still in the low ng region. Precision was found in all cases to be below around 5% for intra-day (repeatability) and below 8.6% for inter-day (reproducibility) studies.

Table 2. Figures of merit for the compounds investigated in this study using H_3O^+ and O_2^+ chemistry. Normalised counts per second for one million reagent ions have been used throughout. Only the dominant ion was used and LoDs were calculated at the E/N value that gave us the best sensitivity. The linear dynamic range in nanograms (ng) is given for each explosive and the corresponding R^2 provided. The precision of the method was evaluated by the determination of the repeatability and reproducibility in terms of percentage of relative standard deviation (% RSD) of peak areas.

COMPOUND	Reagent ion	Monitored ion, m/z	E/N (Td)	Linear dynamic range (ng)	R^2	LoD (pg)	Precision (RSD, %)	
							Repeatability (n=5)	Reproducibility (n=5)
							300 pg	300pg
DPA	H_3O^+	$[\text{DPA.H}]^+$, 170.10	140	0.15-1500	0.9991	72 ± 6	2.9	5.1
	O_2^+	$[\text{DPA}]^+$, 169.09	110		0.9914	$1.4 \pm 0.1^*$	4.9	8.6
2-NO2-DPA	H_3O^+	$[\text{2-NO}_2\text{-DPA H}]^+$, 215.08	140	0.1-1500	0.9998	41 ± 2	2.4	5.2
	O_2^+	$[\text{2-NO}_2\text{-DPA}]^+$, 214.07	80		0.9954	72 ± 5	3.1	6.1
4-NO2-DPA	H_3O^+	$[\text{4-NO}_2\text{-DPA H}]^+$, 215.08	140	0.1-1500	0.9996	51 ± 5	1.5	4.0
	O_2^+	$[\text{2-NO}_2\text{-DPA}]^+$, 214.07	80		0.9941	83 ± 2	2.8	4.5
MC	H_3O^+	$[\text{MC.H}]^+$, 241.13	130	0.2-1500	0.9997	88 ± 4	2.1	3.7
	O_2^+	MC^+ , 240.12	60		0.9965	310 ± 9	3.2	5.1
EC	H_3O^+	$[\text{EC.H}]^+$, 269.17	140	0.15-1500	0.9995	60 ± 7	2.2	4.1
	O_2^+	EC^+ , 268.16	80		0.9955	287 ± 6	3.8	6.3

* expressed in ng. As a result of an endogenous background signal at the mass of interest sensitivity was compromised.

3.3. Application to commercial samples

Six commercial smokeless powders samples from three different manufacturers were analysed. The concentration of additives was calculated using the standard calibration curves obtained for section 3.2. Results, see table 3, show the identified additives and its content in the smokeless gun powder (expressed as percentage) for the different samples for H_3O^+ and O_2^+ reagent ions at 140 Td (a compromise E/N value between high signal intensity and low fragmentation). These results are in good agreement with those found in the smokeless powders database.⁵⁷ Figure 4 shows two mass spectra exemplifying two of the samples for water chemistry - similar plots (not shown) were found for the rest of the samples and for oxygen chemistry.

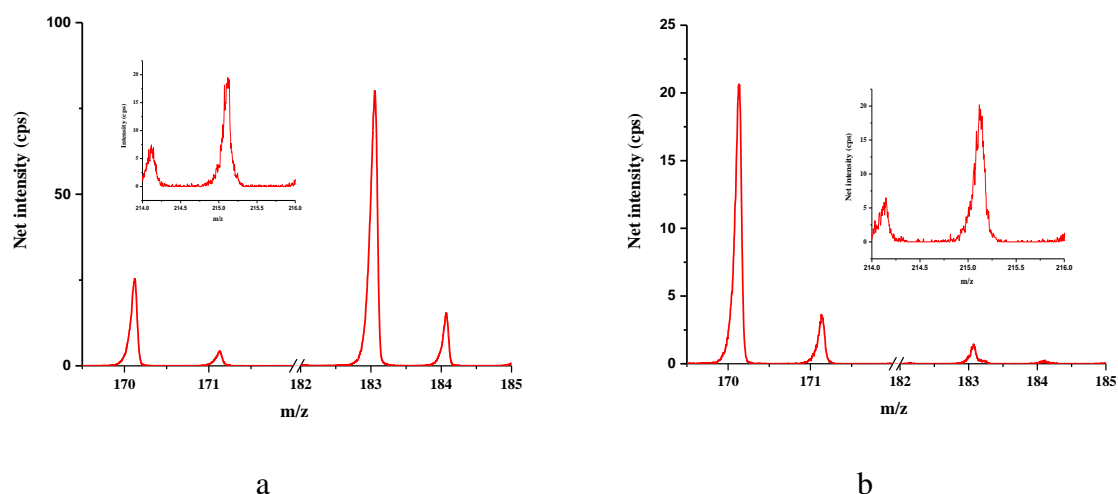


Figure 4. Mass spectra using water chemistry and reduced electric field of 140 Td for (a) IMR4198 and (b) Hodgdon BL-C(2) showing regions around m/z 170 and 215 and the different composition for both powders. (The insertion represents an expansion of the mass range around m/z 215 (x 20).)

Based on our previous water chemistry work,^{41,47,50} and besides the detection of the additives studied for this work, dinitrotoluene was also clearly observed showing two intense product ions peaks at m/z 183.04 and 201.05, assigned to the protonated parent, DNT.H^+ , and its first water cluster, $\text{DNTH}^+.\text{H}_2\text{O}$. This was observed for 3 of the samples. It is possible to assign dinitrotoluene to be the 2,4-isomer. As reported recently by González-Méndez *et al.*^{47,50} monitoring product ions at m/z 183.04 and 201.05 allows assignment to 2,4-DNT, but that the presence of m/z 136.04 (elimination of HONO from the protonated parent) and m/z 91.06 (elimination of two nitro groups) observed at the high E/N setting (200 Td and above) indicates the presence of 2,6-DNT. These two latter peaks were not observed. No detailed product ion

distribution studies for DNT and O_2^+ exist (to the best of our knowledge), but in O_2^+ mode, the charge transfer reaction channel leading to a peak at m/z 182.03 (assigned to $[DNT]^+$) was observed.

The other 3 samples showed an intense peak at m/z 228.03. Fast switching experiments and previous studies dealing with 2,4,6-trinitrotoluene (TNT) and nitroglycerine (NG) confirmed this to be NG.^{41,49,50} NG produces a characteristic signal at m/z 46.01 (NO_2^+) at high E/N values, whilst TNT does not, thus a quick change in the E/N from low (80 Td) to high (180 Td) allows to assign this peak to NG.

Both Alliant powders show evidence of 2,4-DNT and also peaks at m/z 170.10, 215.08, and 269.17, assigned to $[DPA.H]^+$, $[2-,4-NO_2-DPA.H]^+$ and $[EC.H]^+$, respectively. Fast E/N switching experiments confirm the identity of these species based on the presence or absence of fragment ions at different reduced electric fields. Fast switching experiments based on figures 1(a) and 1(b), for both Alliant Red Dot and Unique powder, as shown in Figure 5, confirmed the identity of m/z 215.08 to be the 2-nitrodiphenylamine isomer. The presence or absence of m/z 197.07 and 198.08 would rule out one or another. Also, the presence of m/z 180.06 would confirm the existence of 2- NO_2 -DPA.

For the Hodgdon samples only H322 did show evidences of 2,4-DNT, but BL-C(2) showed a signal at m/z 228.03, assigned again to NG based on fast switching experiments. Both Hodgdon samples showed clear signals at m/z 170.10 and 215.08. Fast switching experiments confirmed m/z 215.08 to be 2-nitrodiphenylamine for Hodgdon-BL-C(2). However, in O_2^+ mode no evidence for 2-nitrodiphenylamine was observed.

Both IMR samples showed a clear and intense peak for 2,4-DNT, and peaks at m/z 170.10, 215.08, 241.13 and 269.17 were also observed. Fast switching experiments confirmed the nitrodiphenylamine to be a mixture of the 2- and 4-isomers.

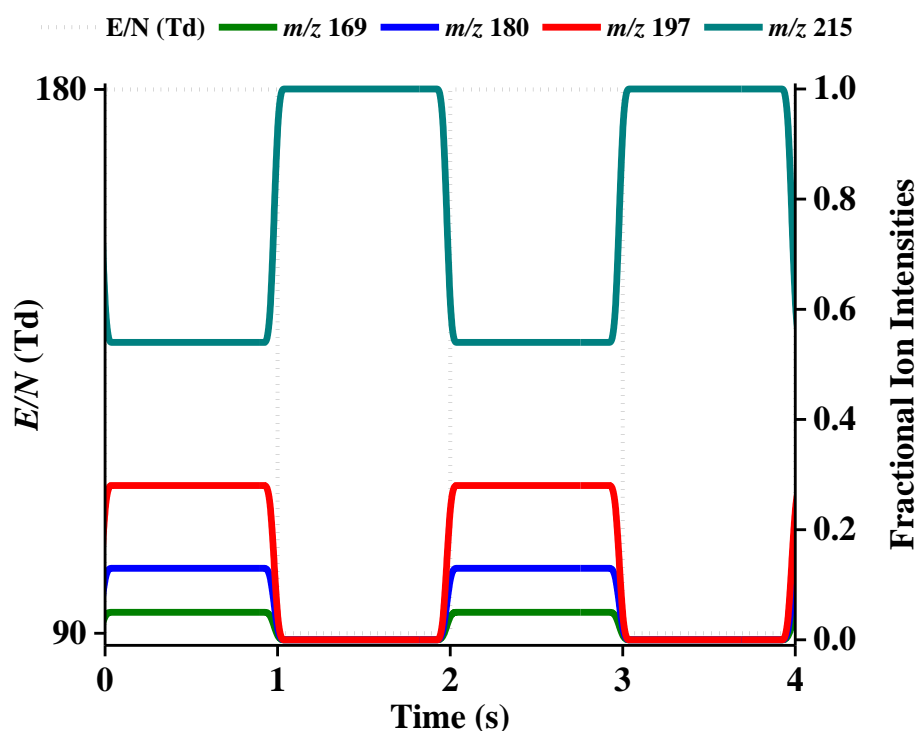


Figure 5. Changes in the fractional ion intensities averaged over each cycle using fast E/N switching experiments at 1 Hz between 90 Td and 180 Td for Alliant Red Dot. The product ions showed are distinctive of 2-NO₂-DPA. The dotted line represents the E/N during each phase.

As stated in the introduction, owing to the complex composition of smokeless powders the presence of unidentified peaks was expected, the majority coming from the plasticizers used in the manufacturing process. This was confirmed by additional unidentified peaks for all the powders at m/z 149.02 (reported by Scherperel *et al.* as a dibutyl phthalate fragment),²⁹ 205.09 and 279.16 (the latter is assigned to be protonated dibutyl phthalate [DBP.H]⁺ by Reese *et al.*,⁸ and Perez *et al.*¹⁵). It is evident that a more detailed study dealing with these is needed if a complete chemical analysis is required.

Table 3. Smokeless powders analysis in H₃O⁺ and O₂⁺ modes at 140 Td, showing the detected (or undetected) additives for six different samples from three different manufacturers. Numbers indicate the content of additive in the powder (in %, mean of n=5) and its error (expressed as RSD).

Smokeless powder manufacturer and model		Reagent ion	DPA	2-NO2-DPA	4-NO2-DPA	MC	EC	2,4-DNT	NG
	Alliant Unique	H ₃ O ⁺	2.0 ± 0.25	1.1 ± 0.2	ND	ND	1.2 ± 0.1	ND ^a	✓ ^b
		O ₂ ⁺	1.6 ± 0.4	0.9 ± 0.3	ND	ND	1.0 ± 0.3	-- ^c	--
	Alliant Red dot	H ₃ O ⁺	2.3 ± 0.2	1.4 ± 0.3	ND	ND	1.1 ± 0.2	ND	✓
		O ₂ ⁺	2.1 ± 0.3	1.0 ± 0.2	ND	ND	0.9 ± 0.2	--	--
	Hodgdon BL-C(2)	H ₃ O ⁺	1.1 ± 0.1	0.6 ± 0.1	ND	ND	3.0 ±	ND	✓
		O ₂ ⁺	0.9 ± 0.1	ND	ND	ND	2.7 ±	--	--
	Hodgdon H322	H ₃ O ⁺	1.6 ± 0.6	0.4 ± 0.2	ND	2.0 ± 0.2	ND	✓	ND
		O ₂ ⁺	1.3 ± 0.4	ND	ND	1.6 ± 0.3	ND	--	--
	IMR 4350	H ₃ O ⁺	4.1 ± 0.3	0.4 ± 0.1	0.6 ± 0.2	2.1 ± 0.3	1.2 ± 0.1	✓	ND ^a
		O ₂ ⁺	4.0 ± 0.5	0.4 ± 0.2	0.4 ± 0.1	1.9 ± 0.2	1.0 ± 0.3	--	--
	IMR 4198	H ₃ O ⁺	5.0 ± 0.1	ND	ND	ND	ND	✓	ND
		O ₂ ⁺	4.7 ± 0.3	ND	ND	ND	ND	--	--

69

70 ^a N.D. indicates not detected; ^b ✓ indicates observed and identified but not quantified and ^c -- indicates not experimentally tested for.

4. Conclusions

We have shown that direct injection soft chemical ionisation-mass spectrometry, using both water and oxygen reagent gases, can analyse smokeless powder organic additives. This has been applied to their identification for commercial powders in their pre-detonation condition.

This method makes use of commercially available swabs and thermal desorption, allowing complete analysis of samples within ~ 10 s. For a series of the most common organic additives for smokeless powders, fragmentation patterns have been established and analytical figures of merit have been reported. Achieving the best LoDs for oxygen chemistry requires using lower reduced electric fields values than those used for water chemistry. Oxygen chemistry has been tested to be less sensitive than water chemistry for the compounds of interest. Fragmentation has been shown to be very similar in terms of the observed ions and their identity for both reagent ions. For H_3O^+ and O_2^+ the most intense ions are usually coming from the non-dissociative channels.

Fast switching experiments aided in the identification and distinguish between isomers, based on the presence or absence of fragment ions at different reduced electric fields.

When applied to commercial samples, results have shown that the content of the organic additives investigated in this study changed between the samples, helping to differentiate among samples and manufacturers.

Future work will include extending the number of additives and plasticisers and commercial samples. Moreover, and also importantly, analysis of post-blast samples to ensure organic gunshot residues can be detected in a rapid, sensitive and selective way using this DI-SCIMS technology. Similarly to recent studies,⁴⁷ the potential use of a radio frequency ion-funnel drift tube to check for improvements in both sensitivity and selectivity is worthwhile to mention.

5. Acknowledgements

RGM is an Early Stage Researcher who acknowledges the support of the PIMMS Initial Training Network which in turn is supported by the European Commission's 7th Framework Programme under Grant Agreement Number 287382.

6. References

1. Heramb, R. M.; McCord, B. R., The manufacture of smokeless powders and their forensic analysis: a brief review. *Forensic Sci. Commun* **2002**, 4 (2).

2. Bender, E. C., Analysis of low explosives. In *Forensic Investigation of Explosions*, Taylor & Francis Ltd., Bristol, PA: 1998.
3. Schwoeble, A.; Exline, D. L., *Current methods in forensic gunshot residue analysis*. CRC Press: 2000.
4. Chang, K. H.; Jayaprakash, P. T.; Yew, C. H.; Abdullah, A. F. L., Gunshot residue analysis and its evidential values: a review. *Australian journal of forensic sciences* **2013**, *45* (1), 3-23.
5. MacCrehan, W. A.; Smith, K. D.; Rowe, W. F., Sampling protocols for the detection of smokeless powder residues using capillary electrophoresis. *Journal of Forensic Science* **1998**, *43* (1), 119-124.
6. Abrego, Z.; Ugarte, A.; Unceta, N.; Fernández-Isla, A.; Goicolea, M. A.; Barrio, R. J., Unambiguous Characterization of Gunshot Residue Particles Using Scanning Laser Ablation and Inductively Coupled Plasma-Mass Spectrometry. *Analytical Chemistry* **2012**, *84* (5), 2402-2409.
7. Dennis, D.-M. K.; Williams, M. R.; Sigman, M. E., Assessing the evidentiary value of smokeless powder comparisons. *Forensic science international* **2016**, *259*, 179-187.
8. Reese, K. L.; Jones, A. D.; Smith, R. W., Characterization of smokeless powders using multiplexed collision-induced dissociation mass spectrometry and chemometric procedures. *Forensic Science International* **2017**, *272*, 16-27.
9. Goudsmits, E.; Sharples, G. P.; Birkett, J. W., Recent trends in organic gunshot residue analysis. *TrAC Trends in Analytical Chemistry* **2015**, *74*, 46-57.
10. Taudte, R. V.; Beavis, A.; Blanes, L.; Cole, N.; Doble, P.; Roux, C., Detection of Gunshot Residues Using Mass Spectrometry. *BioMed Research International* **2014**, *2014*, 16.
11. Dalby, O.; Butler, D.; Birkett, J. W., Analysis of gunshot residue and associated materials—a review. *Journal of forensic sciences* **2010**, *55* (4), 924-943.
12. Joshi, M.; Rigsby, K.; Almirall, J. R., Analysis of the headspace composition of smokeless powders using GC–MS, GC– μ ECD and ion mobility spectrometry. *Forensic Science International* **2011**, *208* (1–3), 29-36.
13. Meng, H.; Caddy, B., Gunshot residue analysis—a review. *Journal of Forensic Science* **1997**, *42* (4), 553-570.
14. Mach, M.; Pallos, A.; Jones, P., Feasibility of gunshot residue detection via its organic constituents. Part I: Analysis of smokeless powders by combined gas chromatography-chemical ionization mass spectrometry. *Journal of Forensic Science* **1978**, *23* (3), 433-445.

15. Perez, J. J.; Watson, D. A.; Levis, R. J., Classification of Gunshot Residue Using Laser Electrospray Mass Spectrometry and Offline Multivariate Statistical Analysis. *Analytical Chemistry* **2016**, 88 (23), 11390-11398.
16. MacCrehan, W. A.; Bedner, M., Development of a smokeless powder reference material for propellant and explosives analysis. *Forensic Science International* **2006**, 163 (1–2), 119-124.
17. Cascio, O.; Trettene, M.; Bortolotti, F.; Milana, G.; Tagliaro, F., Analysis of organic components of smokeless gunpowders: High-performance liquid chromatography vs. micellar electrokinetic capillary chromatography. *ELECTROPHORESIS* **2004**, 25 (10-11), 1543-1547.
18. Meng, H.-h.; Caddy, B., Detection of N,N'-diphenyl-N,N'-diethylurea (ethyl centralite) in gunshot residues using high-performance liquid chromatography with fluorescence detection. *Analyst* **1995**, 120 (6), 1759-1762.
19. López-López, M.; Bravo, J. C.; García-Ruiz, C.; Torre, M., Diphenylamine and derivatives as predictors of gunpowder age by means of HPLC and statistical models. *Talanta* **2013**, 103, 214-220.
20. Laza, D.; Nys, B.; Kinder, J. D.; Kirsch-De Mesmaeker, A.; Moucheron, C., Development of a Quantitative LC-MS/MS Method for the Analysis of Common Propellant Powder Stabilizers in Gunshot Residue*. *Journal of Forensic Sciences* **2007**, 52 (4), 842-850.
21. Wu, Z.; Tong, Y.; Yu, J.; Zhang, X.; Yang, C.; Pan, C.; Deng, X.; Wen, Y.; Xu, Y., The Utilization of MS-MS Method in Detection of GSRs. **2001**.
22. Thomas, J. L.; Lincoln, D.; McCord, B. R., Separation and detection of smokeless powder additives by ultra performance liquid chromatography with tandem mass spectrometry (UPLC/MS/MS). *J Forensic Sci* **2013**, 58 (3), 609-15.
23. López-López, M.; Ferrando, J. L.; García-Ruiz, C., Comparative analysis of smokeless gunpowders by Fourier transform infrared and Raman spectroscopy. *Analytica Chimica Acta* **2012**, 717, 92-99.
24. Zeichner, A.; Eldar, B.; Glatstein, B.; Koffman, A.; Tamiri, T.; Muller, D., Vacuum collection of gunpowder residues from clothing worn by shooting suspects, and their analysis by GC/TEA, IMS, and GC/MS. *Journal of forensic sciences* **2003**, 48 (5), 961-972.
25. Cruces-Blanco, C.; Gámiz-Gracia, L.; García-Campaña, A. M., Applications of capillary electrophoresis in forensic analytical chemistry. *TrAC Trends in Analytical Chemistry* **2007**, 26 (3), 215-226.

26. Bernal Morales, E.; Revilla Vázquez, A. L., Simultaneous determination of inorganic and organic gunshot residues by capillary electrophoresis. *Journal of Chromatography A* **2004**, *1061* (2), 225-233.
27. West, C.; Baron, G.; Minet, J. J., Detection of gunpowder stabilizers with ion mobility spectrometry. *Forensic Science International* **2007**, *166* (2–3), 91-101.
28. Joshi, M.; Delgado, Y.; Guerra, P.; Lai, H.; Almirall, J. R., Detection of odor signatures of smokeless powders using solid phase microextraction coupled to an ion mobility spectrometer. *Forensic Science International* **2009**, *188* (1–3), 112-118.
29. Scherperel, G.; Reid, G. E.; Waddell Smith, R., Characterization of smokeless powders using nanoelectrospray ionization mass spectrometry (nESI-MS). *Analytical and Bioanalytical Chemistry* **2009**, *394* (8), 2019-2028.
30. Wu, Z.; Tong, Y.; Yu, J.; Zhang, X.; Pan, C.; Deng, X.; Xu, Y.; Wen, Y., Detection of N,N[prime or minute]-diphenyl-N,N[prime or minute]-dimethylurea (methyl centralite) in gunshot residues using MS-MS method. *Analyst* **1999**, *124* (11), 1563-1567.
31. Tong, Y.; Wu, Z.; Yang, C.; Yu, J.; Zhang, X.; Yang, S.; Deng, X.; Xu, Y.; Wen, Y., Determination of diphenylamine stabilizer and its nitrated derivatives in smokeless gunpowder using a tandem MS method. *Analyst* **2001**, *126* (4), 480-484.
32. Perez, J. J.; Flanigan, P. M.; Brady, J. J.; Levis, R. J., Classification of Smokeless Powders Using Laser Electrospray Mass Spectrometry and Offline Multivariate Statistical Analysis. *Analytical Chemistry* **2013**, *85* (1), 296-302.
33. Zhao, M.; Zhang, S.; Yang, C.; Xu, Y.; Wen, Y.; Sun, L.; Zhang, X., Desorption Electrospray Tandem MS (DESI-MSMS) Analysis of Methyl Centralite and Ethyl Centralite as Gunshot Residues on Skin and Other Surfaces. *Journal of Forensic Sciences* **2008**, *53* (4), 807-811.
34. Morelato, M.; Beavis, A.; Ogle, A.; Doble, P.; Kirkbride, P.; Roux, C., Screening of gunshot residues using desorption electrospray ionisation–mass spectrometry (DESI–MS). *Forensic Science International* **2012**, *217* (1–3), 101-106.
35. Li, F.; Tice, J.; Musselman, B. D.; Hall, A. B., A method for rapid sampling and characterization of smokeless powder using sorbent-coated wire mesh and direct analysis in real time - mass spectrometry (DART-MS). *Science & Justice* **2016**, *56* (5), 321-328.
36. Mahoney, C. M.; Gillen, G.; Fahey, A. J., Characterization of gunpowder samples using time-of-flight secondary ion mass spectrometry (TOF-SIMS). *Forensic science international* **2006**, *158* (1), 39-51.

37. Bueno, J.; Sikirzhyski, V.; Lednev, I. K., Raman spectroscopic analysis of gunshot residue offering great potential for caliber differentiation. *Analytical chemistry* **2012**, 84 (10), 4334-4339.
38. Andrew M. Ellis, C. A. Mayhew, *Proton Transfer Reaction Mass Spectrometry: Principles and Applications*. 1st ed.; Wiley: 2014.
39. Biasioli, F.; Yeretdzian, C.; Märk, T. D.; Dewulf, J.; Van Langenhove, H., Direct-injection mass spectrometry adds the time dimension to (B)VOC analysis. *TrAC Trends in Analytical Chemistry* **2011**, 30 (7), 1003-1017.
40. Lindinger, W.; Hirber, J.; Paretzke, H., An ion/molecule-reaction mass spectrometer used for on-line trace gas analysis. *International Journal of Mass Spectrometry and Ion Processes* **1993**, 129, 79-88.
41. González-Méndez, R.; Reich, D. F.; Mullock, S. J.; Corlett, C. A.; Mayhew, C. A., Development and use of a thermal desorption unit and proton transfer reaction mass spectrometry for trace explosive detection: Determination of the instrumental limits of detection and an investigation of memory effects. *International Journal of Mass Spectrometry* **2015**, 385, 13-18.
42. Shen, C.; Li, J.; Han, H.; Wang, H.; Jiang, H.; Chu, Y., Triacetone triperoxide detection using low reduced-field proton transfer reaction mass spectrometer. *International Journal of Mass Spectrometry* **2009**, 285 (1-2), 100-103.
43. Mayhew, C. A.; Sulzer, P.; Petersson, F.; Haidacher, S.; Jordan, A.; Märk, L.; Watts, P.; Märk, T. D., Applications of proton transfer reaction time-of-flight mass spectrometry for the sensitive and rapid real-time detection of solid high explosives. *International Journal of Mass Spectrometry* **2010**, 289 (1), 58-63.
44. Jürschik, S.; Sulzer, P.; Petersson, F.; Mayhew, C. A.; Jordan, A.; Agarwal, B.; Haidacher, S.; Seehauser, H.; Becker, K.; Märk, T. D., Proton transfer reaction mass spectrometry for the sensitive and rapid real-time detection of solid high explosives in air and water. *Analytical and Bioanalytical Chemistry* **2010**, 398 (7-8), 2813-2820.
45. Sulzer, P.; Agarwal, B.; Jürschik, S.; Lanza, M.; Jordan, A.; Hartungen, E.; Hanel, G.; Märk, L.; Märk, T. D.; González-Méndez, R.; Watts, P.; Mayhew, C. A., Applications of switching reagent ions in proton transfer reaction mass spectrometric instruments for the improved selectivity of explosive compounds. *International Journal of Mass Spectrometry* **2013**, 354-355 (0), 123-128.
46. Agarwal, B.; González-Méndez, R.; Lanza, M.; Sulzer, P.; Märk, T. D.; Thomas, N.; Mayhew, C. A., Sensitivity and Selectivity of Switchable Reagent Ion Soft Chemical

237 Ionization Mass Spectrometry for the Detection of Picric Acid. *The Journal of Physical*
 238 *Chemistry A* **2014**, *118* (37), 8229-8236.

239 47. González-Méndez, R.; Watts, P.; Olivenza-León, D.; Reich, D. F.; Mullock, S. J.;
 240 Corlett, C. A.; Cairns, S.; Hickey, P.; Brookes, M.; Mayhew, C. A., Enhancement of
 241 Compound Selectivity Using a Radio Frequency Ion-Funnel Proton Transfer Reaction Mass
 242 Spectrometer: Improved Specificity for Explosive Compounds. *Analytical Chemistry* **2016**,
 243 *88* (21), 10624-10630.

244 48. González-Méndez, R. Development and applications of Proton Transfer Reaction-Mass
 245 Spectrometry for Homeland Security: trace detection of explosives. PhD, University of
 246 Birmingham, 2017.

247 49. Sulzer, P.; Petersson, F.; Agarwal, B.; Becker, K. H.; Jürschik, S.; Märk, T. D.; Perry,
 248 D.; Watts, P.; Mayhew, C. A., Proton Transfer Reaction Mass Spectrometry and the
 249 Unambiguous Real-Time Detection of 2,4,6 Trinitrotoluene. *Analytical Chemistry* **2012**, *84*
 250 (9), 4161-4166.

251 50. González-Méndez, R.; Watts, P.; Reich, D. F.; Mullock, S. J.; Cairns, S.; Hickey, P.;
 252 Brookes, M.; Mayhew, C. A., Use of Rapid Reduced Electric Field Switching to Enhance
 253 Compound Specificity for Proton Transfer Reaction-Mass Spectrometry. *Analytical*
 254 *Chemistry* **2018**.

255 51. Eiceman, G. A.; Karpas, Z.; Hill Jr, H. H., *Ion mobility spectrometry*. CRC press: 2013.

256 52. Blake, R. S.; Monks, P. S.; Ellis, A. M., Proton-Transfer Reaction Mass Spectrometry.
 257 *Chemical Reviews* **2009**, *109* (3), 861-896.

258 53. Jordan, A.; Haidacher, S.; Hanel, G.; Hartungen, E.; Herbig, J.; Märk, L.;
 259 Schottkowsky, R.; Seehauser, H.; Sulzer, P.; Märk, T. D., An online ultra-high sensitivity
 260 Proton-transfer-reaction mass-spectrometer combined with switchable reagent ion capability
 261 (PTR + SRI – MS). *International Journal of Mass Spectrometry* **2009**, *286* (1), 32-38.

262 54. Harrison, A. G., *Chemical Ionization Mass Spectrometry*. CRC Press: 1982.

263 55. Gross, J. H., *Mass Spectrometry. A textbook*. 2nd ed.; Springer: 2011.

264 56. Gilbert-López, B.; García-Reyes, J. F.; Ortega-Barrales, P.; Molina-Díaz, A.;
 265 Fernández-Alba, A. R., Analyses of pesticide residues in fruit-based baby food by liquid
 266 chromatography/electrospray ionization time-of-flight mass spectrometry. *Rapid*
 267 *communications in mass spectrometry* **2007**, *21* (13), 2059-2071.

268 57. The Smokeless Powders Database <http://www.ilrc.ucf.edu/powders/index.php>
 269 (accessed 08-03-2018).